

Dynamic formation of arrays of interacting optical spatial solitons under light-sheet illumination

OTO BRZOBHATÝ^{1,*}, LUKÁŠ CHVÁTAL¹, ALEXANDR JONÁŠ¹, AND PAVEL ZEMÁNEK¹

¹ The Czech Academy of Sciences, Institute of Scientific Instruments, Královopolská 147, 612 64 Brno, Czech Republic

*otobrz@isibrno.cz

Compiled March 7, 2025

Colloidal suspensions of micron- and submicron-sized particles act as effective nonlinear media that can self-arrange into intricate static or dynamic structures upon illumination with a laser beam. Optical spatial solitons (OSSs) represent a prominent example of such light-induced structures. We study the formation of two-dimensional arrays of interacting OSSs from colloidal particles of varying sizes illuminated by counter-propagating light-sheet beams. We monitor evolution of growing OSS arrays upon addition of individual constituent particles and show that a small change in the total number of particles in the structure can induce long-range reconfiguration of the overall OSS layout. In particular, the minimal distance between the neighboring OSSs in the array is observed to nearly linearly increase with increasing number of constituent particles. Our experimental observations are semi-quantitatively supported by theoretical modeling based on the rigorous multiple Mie scattering theory.

<http://dx.doi.org/10.1364/ao.XX.XXXXXX>

Controlled exchange of momentum between light and matter has been employed for both stable spatial confinement and dynamic driving of motion of micron- and submicron-sized particles suspended in liquid or gaseous environments, with experimental applications in research fields ranging from physics through chemistry to biology [1, 2]. Optical manipulations typically exploit carefully shaped incident laser beams that generate well-defined external force fields capable of capturing or moving illuminated particles along desired trajectories [1, 2]. In contrast to such predefined force fields, dynamic landscapes of optical forces can arise due to complex two-way interactions between the incident light and illuminated particles that cause modulations of the intensity profile of the incident light wave. For particles much smaller than the incident light wavelength (Rayleigh scatterers), this light-matter interaction predominantly results from the local spatial gradients of optical intensity that tend to pull particles optically denser than the ambient medium to the place of maximal intensity [3]. On the other hand, for larger particles that strongly scatter the incident light, dynamic forces that drive the particle motion originate primarily in the interference between the incident and scattered light waves, leading to

so-called optical binding in which both gradient and scattering forces in the resulting interference pattern are relevant [4].

In general, the above described light-matter interactions are nonlinear and can lead to emergence of complex, non-intuitive static or dynamic self-assembled structures. A prominent example of such pattern formation are optical spatial solitons (OSSs), spatially localized, non-diffracting modes supported in nonlinear optical media [5]. Formation of OSSs in colloidal suspensions has been studied both theoretically [6–8] and experimentally [9–11] and application of OSSs in reconfigurable optofluidic waveguiding has been demonstrated [12]. Depending on the size of the constituent particles, OSS formation can be described using either the model of an effective continuous medium with a spatially varying refractive index [6–8], which extends down to the scale of degenerate quantum gases [13], or the framework of optical binding that takes into account discreteness of the system resulting in enhanced light scattering effects [4].

As shown recently, non-conservative character of optical binding interactions causes inherent instability of optically bound clusters with increasing number of constituent particles [14]. In particular, the influx of momentum from the illuminating light beam that is asymmetrically redistributed by multiple scattering events inevitably leads to the emergence of unstable modes of collective motion of optically bound structures. Such behavior has indeed been experimentally observed and interpreted in terms of non-pairwise character of optical binding forces [15]. Despite this progress, systematic characterization of dynamically formed, mutually interacting OSSs under well controlled conditions of self-assembly remains a formidable task.

In this Letter, we report on a systematic study of formation of arrays of OSSs from colloidal particles of varying sizes illuminated by counter-propagating light-sheet beams generated by a spatial light modulator (SLM). The light-sheet illumination geometry [16] with on-the-fly adjustable profiles of the beams allows us to confine the optically bound OSS arrays to two dimensions (2D) by the strong gradient forces acting along the light sheet thickness [y axis; see Fig 1(a)], which greatly facilitates the observation of positions of all constituent particles during the process of OSS array formation. We monitor the evolution of growing OSS arrays upon addition of individual constituent particles and show that a small change in the total number of particles in the structure can induce long-range reconfiguration of the overall OSS layout. Our experimental observations are semi-quantitatively supported by theoretical modeling based on

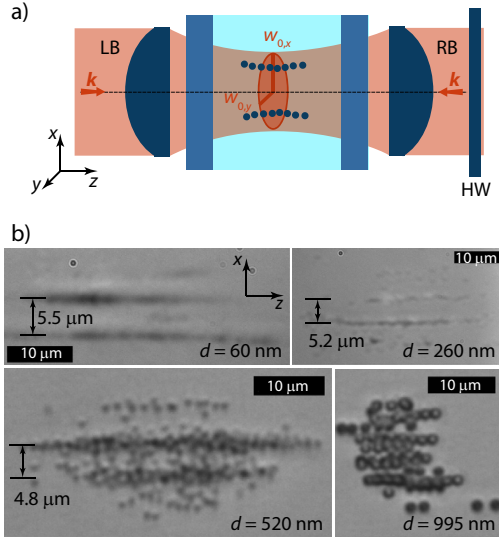


Fig. 1. (a) Dual-beam optical trap formed by two linearly polarized, counter-propagating light-sheet laser beams (LB and RB) with orthogonal polarization controlled by a half-wave plate (HW). Optically trapped and bound particles located in the plane of the light sheet (the xz -plane) are observed using a microscope oriented along the y -axis. (b) Polystyrene particles of various diameters d self-assembled into arrays of parallel OSSs upon illumination with C-P light-sheet beams with fixed beam-waist radii of $w_{0,x} = 10.5 \mu\text{m}$ and $w_{0,y} = 1.6 \mu\text{m}$.

the rigorous multiple Mie scattering theory.

In our experiments, we employed a dual-beam optical trap formed by two counter-propagating (C-P) light-sheet beams (wavelength 1064 nm) with orthogonal linear polarization, overlapping inside a vertically oriented glass capillary with square cross-section (inner dimensions $100 \times 100 \mu\text{m}$). The capillary was filled with a suspension of monodisperse polystyrene microspheres (refractive index 1.59) in deionized water. In the experiments, the microsphere diameter d varied between 60 – 995 nm. Using an SLM, we created focused light-sheet beams with transverse beam-waist radii of $w_{0,x} = (10.5 \pm 0.1) \mu\text{m}$ and $w_{0,y} = (1.6 \pm 0.1) \mu\text{m}$. The trapping power of each beam just outside the capillary was set to $\sim 125 \text{ mW}$ by controlling the power of the trapping laser. Resulting quasi-planar self-assembled colloidal structures were observed by an optical microscope from a direction perpendicular to the plane of the light sheet (the y -direction), see Fig 1(a). Detailed description of the experimental setup can be found in Section 1 of Supplement 1.

As illustrated in Fig. 1(b), upon illuminating aqueous suspensions of polystyrene particles of varying diameters indicated in the images with cross-polarized C-P light-sheet beams, we observed the formation of multiple parallel chains of particles confined in the plane of the light sheet. These structures corresponded to quasi-planar 2D arrays of OSSs [9]. Inspection of Fig. 1(b) reveals that the spacing of neighboring chains monotonically decreased with increasing particle size (for 995 nm particles, a single characteristic spacing is not well defined). As argued in [9], this effect can be attributed to the increasing importance of the granular nature of the effective nonlinear medium represented by the colloidal suspension in which the OSSs are formed. This implies that the continuous-medium approach, appropriate for modeling suspensions of nanoparticles [9, 11], gradually breaks down and multiple scattering events that lead to optical

binding start dominating the process of self-organization. As indicated by direct visual inspection of the recorded images, with increasing particle size, individual constituent particles forming the OSSs become more regularly arranged by the optical binding forces, reflecting the spatial distribution of the interference maxima in which the particles are preferentially confined [4].

The process of formation of an OSS array from polystyrene particles with the diameter of 657 nm is depicted in Fig. 2(a). Initially, optical binding forces induce self-assembly of illuminated particles into a single linear chain with non-equidistant spacing between neighboring particles located on the axis of symmetry of the light-sheet beams (optical axis) [12] (top panel). With growing size of the primary OSS chain, the complexity of the force landscape created due to multiple scattering events from this chain increases, eventually leading to formation of new stable trapping positions away from the optical axis, which subsequently serve as nucleation sites for the second and additional parallel linear OSS structures (middle and bottom panels).

The phenomenon of optical binding, triggered by multiple scattering of light, depends not only on the properties of the illuminated objects, i.e., their shape [17, 18], material [19], or internal structure [20], but also on the spatial profile of the incident field [21, 22] and its polarization [23]. Moreover, intensity of the scattered field and, consequently, stability of the secondary off-axis optical traps are also influenced by the number of particles in the primary on-axis chain. Generally, for the given particle size and material, the number of stable off-axis traps increases with growing length of the primary chain. However, once the number of particles in this chain reaches a critical value (determined by the particle size and refractive index and by the transverse intensity profiles of the trapping beams) for which the trapping beams are not allowed to propagate through the structure [12], the structure becomes unstable and starts oscillating and dynamically rearranging [24, 25]. For a larger particle size, this dynamic structural instability occurs at a smaller total number of particles in the structure; it represents the effect of increasingly more non-conservative binding forces acting along the directions both parallel and perpendicular to the propagation axes of the light-sheet beams [14].

Figure 2(b) shows trajectories of individual particles diffusing one by one towards an already formed primary OSS. These particles eventually joined the OSS structure aligned along the red dashed line. Position histogram in Fig. 2(c) then quantitatively summarizes the motion of the particles from Fig. 2(b), with yellow color indicating the region of the highest 2D probability density of particles' occurrence where the secondary OSS is most likely to form. After applying the Boltzmann statistics to the position histogram 2(c) [26], it could be converted to an effective potential landscape created in the vicinity of the primary OSS due to the interference of the incident and scattered fields. This analysis revealed that the deepest trap, in which the particles remained transiently confined for the longest time, was created at $x \approx \pm 2.5 \mu\text{m}$ away from the center of the OSS structure located at $[x, z] = [0, 0] \mu\text{m}$.

To corroborate our experimental observations, we carried out numerical simulations of the formation of additional particle chains in the vicinity of existing OSS structures with varying numbers of constituent particles (see Section 2 of Supplement 1 for the details of the simulation methodology). The simulation parameters were chosen to reflect the real experimental system, i.e., particle diameter 657 nm, particle refractive index 1.59, aqueous ambient medium with refractive index 1.33, and beam waist radii of the light-sheet beams $w_{0,x} = 10.5 \mu\text{m}$ and $w_{0,y} = 1.6 \mu\text{m}$.

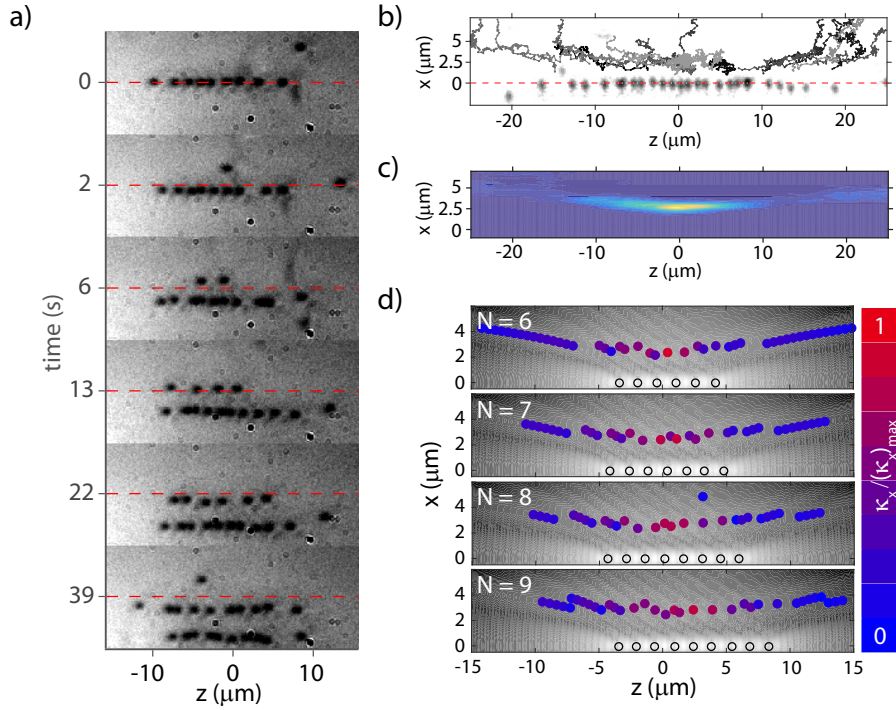


Fig. 2. (a) (top to bottom) Time evolution of the formation of parallel OSSs from polystyrene particles of diameter 657 nm illuminated by C-P light-sheet beams. Red dashed lines mark the optical axis. (b) Transient trajectories of particles diffusing in the vicinity of an OSS originally formed from 15 particles along the red dashed line and centered at $[x, z] = [0, 0]$ μm . Each trajectory corresponds to a single particle approaching the OSS, serving as a probe of the local force field before it joins the OSS and increases the number of particles in the structure by one (see Section 4 of Supplement 1 for details on the determination of local optical forces from the recorded particle trajectories). (c) 2D histogram of positions obtained from the ensemble of trajectories shown in (b). The yellow region centered at $[x, z] = [2.5, 0]$ μm indicates the area of the highest probability density of particle occurrence, i.e., a local minimum of the optical potential landscape where a secondary OSS is most likely to nucleate. (d) Simulations of the formation of secondary optical traps in the vicinity of OSSs with varying numbers of constituent particles N . The grayscale background visualizes the simulated spatial profile of the net optical intensity around the primary on-axis OSS (empty circles), colored circles indicate individual secondary trapping locations whose normalized lateral stiffness $\kappa_x/(\kappa_x)_{\text{max}}$ is color encoded [$(\kappa_x)_{\text{max}}$: maximal value of κ_x for all considered N]. Experimental and simulation parameters: particle diameter 657 nm, particle refractive index 1.59, ambient refractive index 1.33, beam waist radii of the light-sheet beams $w_{0,x} = 10.5$ μm , $w_{0,y} = 1.6$ μm .

The number of particles in the primary OSS structure N then varied as $N = 6 - 9$. Initially, we found a stable configuration of the linear chain of N self-arranged particles in the primary on-axis OSS. Subsequently, we moved a single probe particle along a regular 2D grid surrounding the primary OSS, determined the value of $F^{\text{opt}}(x, z)$ exerted on the probe particle at the given location $[x, z]$, and evaluated the trap stiffness κ_x, κ_z along the x and z axes at the tentative secondary trapping positions (see Supplement 1 for details).

Figure 2(d) summarizes the results of the simulations described above. Specifically, individual panels show the spatial profiles of intensity of the net optical field (grayscale background) formed in the vicinity of the primary OSS chains of varying length (empty circles). The colored circles then mark possible off-axis trapping locations created in the net optical field around the primary OSS. Asymmetry of these trapping locations with respect to $z = 0$ results from orthogonal polarization of the two C-P light-sheet beams. To facilitate quantitative assessment, the normalized lateral stiffness $\kappa_x/(\kappa_x)_{\text{max}}$ of the secondary traps, which characterizes the strength of interaction between the parallel chains in the OSS structure, is color-encoded, with red color indicating maximal stiffness and blue color indicating

minimal stiffness. In general, off-axis traps with a higher value of κ_x are more likely to function as stable nucleation sites for the secondary OSS chains. Overall, the simulated shape of the secondary trapping domain is very similar to the experimentally observed profiles presented in Fig. 2(b) and 2(c). As shown in Section 3 of Supplement 1, the configuration of 2D OSS arrays is rather sensitive to the size of the constituent particles. This feature directly reflects the complex landscapes of optical binding forces that exist in the interference field between the incident and scattered light and that can greatly vary near the resonant scattering conditions. Using the stochastic simulations, it is possible to quantitatively characterize the formation of the dynamic 2D OSS structures under fully controlled conditions, which would be rather challenging to achieve in the experiments.

Inspection of numerically found off-axis trapping positions around the OSSs containing 6 – 9 particles reveals that the predicted positions of these secondary traps shift farther from the on-axis OSS with increasing number of particles in the structure [see Fig. 2(d)]. To verify this prediction, we experimentally studied the minimal separation distance Δx between the adjacent OSSs as a function of the total number of particles in the structure, N_{total} . Figure 3 shows the evolution of Δx for two

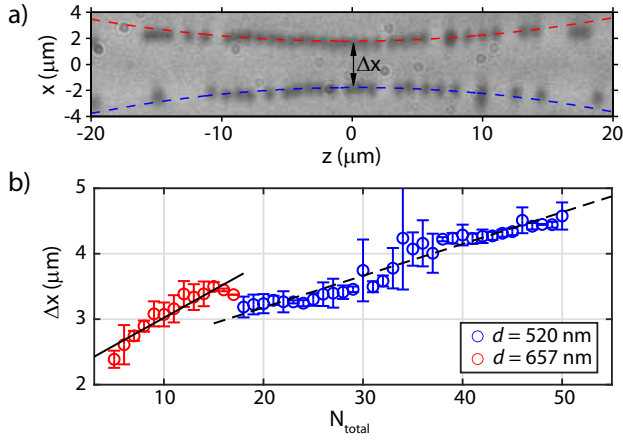


Fig. 3. Dependence of lateral spacing in OSS arrays on the total number of constituent particles N_{total} . (a) Polystyrene particles (diameter 520 nm, $N_{\text{total}} = 50$) self-assembled into two parallel OSS chains upon illumination with two C-P light-sheet beams (beam waist radii $w_{0,x} = 10.5 \mu\text{m}$ and $w_{0,y} = 1.6 \mu\text{m}$). Δx defines the minimal separation distance of the adjacent OSSs determined using parabolic fits of positions of particles in the top and the bottom chain (dashed lines). (b) Experimentally determined dependence of Δx on N_{total} for polystyrene particles of two different diameters (520 nm and 657 nm). Solid and dashed line denote the respective linear fits to the experimental data. The data points and error bars were determined from 10 independent records of OSS formation.

parallel OSS chains of varying length gradually formed in C-P light-sheet beams from particles of two different diameters (520 nm and 657 nm). Careful adjustment of particle concentration allowed observing discrete elongation events represented by addition of individual particles to the existing OSS structures. Within the studied ranges of N_{total} , the values of Δx were observed to nearly linearly increase with N_{total} . The measured slope of the dependence of Δx on N_{total} for the larger 657 nm particles was then 1.74-times bigger than the corresponding slope for the smaller 520 nm particle. This is expected, as the larger particles act as stronger scattering centers and, thus, addition of a single particle to the OSS structure has a more profound effect on its overall configuration. Also, OSSs formed from larger particles start displaying dynamic instability for a smaller value of N_{total} [12]. From Fig. 3(a), it is evident that OSSs with extended length tend to be curved [compare with Fig. 1(b) and 2(a)]. This feature results from the spatial variation of the local width of the light-sheet beams along the x -axis as the beams propagate along the z -axis [compare also with the simulations in Fig. 2(d)].

In conclusion, we have systematically characterized the formation of 2D OSS arrays in colloidal suspensions with varying particle sizes illuminated with two C-P light-sheet beams. Our observations indicate that the structure and stability of such OSS arrays is strongly influenced by the number and size of the constituent particles. In contrast to the surface-assisted 2D experimental geometry used in [9, 27], our 2D OSS arrays are held in bulk solution solely by the forces of light. Thus, light-particle interactions can be studied in isolation from surface effects induced by the proximity of the sample chamber walls. Adjustment of the beam waist radii of the incident light-sheet beams generated by an SLM then, in principle, allows controlling the

configuration of the self-assembled OSS structures and characterizing their response to changes in external optical forces [12, 22]. The reported results pave the way to the development of an experimental toolbox for characterizing the optomechanics of complex coupled systems with the level of coupling nonlinearity controlled by shaping of the incident optical field, potentially applicable in designing novel mesoscopic-scale photonic devices whose spectral or polarization response can be reconfigured in situ by light.

Funding. EC and Ministerstvo školství, mládeže a tělovýchovy (CZ.02.01.01/00/22_008/0004649, O.B.); The Czech Science Foundation (24-11503S, A.J.); Akademie věd České republiky (Praemium Academiae, P.Z.).

Disclosures. The authors declare no conflicts of interest.

Data Availability Statement. Data underlying the results presented in this paper are not publicly available at this time but may be obtained from the authors upon reasonable request.

Supplemental document. See Supplement 1 for supporting content.

REFERENCES

- J. Gieseler, J. R. Gomez-Solano, A. Magazzu, *et al.*, *Adv. Opt. Photonics* **13**, 74 (2021).
- P. Zemánek, G. Volpe, A. Jonáš, and O. Brzobohatý, *Adv. Opt. Photonics* **11**, 577 (2019).
- Y. Harada and T. Asakura, *Opt. Commun.* **124**, 529 (1996).
- K. Dholakia and P. Zemánek, *Rev. Mod. Phys.* **82**, 1767 (2010).
- G. I. Stegeman and M. Segev, *Science* **286**, 1518 (1999).
- C. Conti, G. Ruocco, and S. Trillo, *Phys. Rev. Lett.* **95**, 183902 (2005).
- R. Gordon, J. T. Blakely, and D. Sinton, *Phys. Rev. A* **75**, 055801 (2007).
- M. Matuszewski, W. Krolikowski, and Y. S. Kivshar, *Phys. Rev. A* **79**, 023814 (2009).
- P. J. Reece, E. M. Wright, and K. Dholakia, *Phys. Rev. Lett.* **98**, 203902 (2007).
- A. Bezryadina, T. Hansson, R. Gautam, *et al.*, *Phys. Rev. Lett.* **119**, 058101 (2017).
- O. Brzobohatý, L. Chvátal, M. Šiler, and P. Zemánek, *Opt. Express* **28**, 37700 (2020).
- O. Brzobohatý, L. Chvátal, A. Jonáš, *et al.*, *ACS Photonics* **6**, 403 (2019).
- G. R. M. Robb, J. G. M. Walker, G.-L. Oppo, and T. A. Ackemann, *Phys. Rev. Res.* **5**, L032004 (2023).
- X. Li, Y. Liu, Z. Lin, *et al.*, *Nat. Commun.* **12**, 6597 (2021).
- D. J. Davenport and D. Kleckner, *Soft Matter* **18**, 4464 (2022).
- O. E. Olarte, J. Andilla, E. J. Gualda, and P. Loza-Alvarez, *Adv. Opt. Photonics* **10**, 111 (2018).
- O. Brzobohatý, A. V. Arzola, M. Šiler, *et al.*, *Opt. Express* **23**, 7273 (2015).
- S. H. Simpson, P. Zemánek, O. M. Maragò, *et al.*, *Nano Lett.* **17**, 3485 (2017).
- V. Demergis and E.-L. Florin, *Nano Lett.* **12**, 5756 (2012).
- O. Brzobohatý, R. J. Hernández, S. Simpson, *et al.*, *Opt. Express* **24**, 26382 (2016).
- T. Čížmár, O. Brzobohatý, K. Dholakia, and P. Zemánek, *Laser Phys. Lett.* **8**, 50 (2011).
- O. Brzobohatý, V. Karásek, T. Čížmár, and P. Zemánek, *Appl. Phys. Lett.* **99**, 101105 (2011).
- C. D. Mellor, T. A. Fennerty, and C. D. Bain, *Opt. Express* **14**, 10079 (2006).
- J. M. Taylor and G. D. Love, *Phys. Rev. A* **80**, 053808 (2009).
- S. A. Tatarkova, A. E. Carruthers, and K. Dholakia, *Phys. Rev. Lett.* **89**, 283901 (2002).
- E. L. Florin, A. Pralle, E. H. K. Stelzer, and J. K. H. Horber, *Appl. Phys. A-Materials Sci. & Process.* **66**, S75 (1998).
- C. D. Mellor and C. D. Bain, *Chem. Phys. Chem.* **7**, 329 (2006).

FULL REFERENCES

1. J. Gieseler, J. R. Gomez-Solano, A. Magazzu, I. P. Castillo, L. P. Garcia, M. Gironella-Torrent, X. Viader-Godoy, F. Ritort, G. Pesce, A. Arzola, K. Volke-Sepulveda, and G. Volpe, "Optical tweezers - from calibration to applications: a tutorial," *Adv. Opt. Photonics* **13**, 74–241 (2021).
2. P. Zemánek, G. Volpe, A. Jonáš, and O. Brzobohatý, "Perspective on light-induced transport of particles: from optical forces to phoretic motion," *Adv. Opt. Photonics* **11**, 577–678 (2019).
3. Y. Harada and T. Asakura, "Radiation forces on a dielectric sphere in the Rayleigh scattering regime," *Opt. Commun.* **124**, 529–541 (1996).
4. K. Dholakia and P. Zemánek, "Colloquium: Grippled by light: Optical binding," *Rev. Mod. Phys.* **82**, 1767–1791 (2010).
5. G. I. Stegeman and M. Segev, "Optical spatial solitons and their interactions: Universality and diversity," *Science* **286**, 1518–1523 (1999).
6. C. Conti, G. Ruocco, and S. Trillo, "Optical spatial solitons in soft matter," *Phys. Rev. Lett.* **95**, 183902 (2005).
7. R. Gordon, J. T. Blakely, and D. Sinton, "Particle-optical self-trapping," *Phys. Rev. A* **75**, 055801 (2007).
8. M. Matuszewski, W. Krolikowski, and Y. S. Kivshar, "Soliton interactions and transformations in colloidal media," *Phys. Rev. A* **79**, 023814 (2009).
9. P. J. Reece, E. M. Wright, and K. Dholakia, "Experimental Observation of Modulation Instability and Optical Spatial Soliton Arrays in Soft Condensed Matter," *Phys. Rev. Lett.* **98**, 203902 (2007).
10. A. Bezryadina, T. Hansson, R. Gautam, B. Wetzel, G. Siggins, A. Kalmbach, J. Lamstein, D. Gallardo, E. J. Carpenter, A. Ichimura, R. Morandotti, and Z. Chen, "Nonlinear Self-Action of Light through Biological Suspensions," *Phys. Rev. Lett.* **119**, 058101 (2017).
11. O. Brzobohatý, L. Chvátal, M. Šiler, and P. Zemánek, "Complex colloidal structures with non-linear optical properties formed in an optical trap," *Opt. Express* **28**, 37700 (2020).
12. O. Brzobohatý, L. Chvátal, A. Jonáš, M. Šiler, J. Kaňka, J. Ježek, and P. Zemánek, "Tunable Soft-Matter Optofluidic Waveguides Assembled by Light," *ACS Photonics* **6**, 403–410 (2019).
13. G. R. M. Robb, J. G. M. Walker, G.-L. Oppo, and T. A. Ackemann, "Long-range interactions in a quantum gas mediated by diffracted light," *Phys. Rev. Res.* **5**, L032004 (2023).
14. X. Li, Y. Liu, Z. Lin, J. Ng, and C. T. Chan, "Non-Hermitian physics for optical manipulation uncovers inherent instability of large clusters," *Nat. Commun.* **12**, 6597 (2021).
15. D. J. Davenport and D. Kleckner, "Formation of colloidal chains and driven clusters with optical binding," *Soft Matter* **18**, 4464–4474 (2022).
16. O. E. Olarte, J. Andilla, E. J. Gualda, and P. Loza-Alvarez, "Light-sheet microscopy: a tutorial," *Adv. Opt. Photonics* **10**, 111 (2018).
17. O. Brzobohatý, A. V. Arzola, M. Šiler, L. Chvátal, P. Ják, S. Simpson, and P. Zemánek, "Complex rotational dynamics of multiple spheroidal particles in a circularly polarized, dual beam trap," *Opt. Express* **23**, 7273–7287 (2015).
18. S. H. Simpson, P. Zemánek, O. M. Maragò, P. H. Jones, and S. Hanna, "Optical Binding of Nanowires," *Nano Lett.* **17**, 3485–3492 (2017).
19. V. Demergis and E.-L. Florin, "Ultrastrong Optical Binding of Metallic Nanoparticles," *Nano Lett.* **12**, 5756–5760 (2012).
20. O. Brzobohatý, R. J. Hernández, S. Simpson, A. Mazzulla, G. Cipparone, and P. Zemánek, "Chiral particles in the dual-beam optical trap," *Opt. Express* **24**, 26382–26391 (2016).
21. T. Čižmár, O. Brzobohatý, K. Dholakia, and P. Zemánek, "The holographic optical micro-manipulation system based on counter-propagating beams," *Laser Phys. Lett.* **8**, 50–56 (2011).
22. O. Brzobohatý, V. Karásek, T. Čižmár, and P. Zemánek, "Dynamic size tuning of multidimensional optically bound matter," *Appl. Phys. Lett.* **99**, 101105 (2011).
23. C. D. Mellor, T. A. Fennerty, and C. D. Bain, "Polarization effects in optically bound particle arrays," *Opt. Express* **14**, 10079–10088 (2006).
24. J. M. Taylor and G. D. Love, "Spontaneous symmetry breaking and circulation by optically bound microparticle chains in Gaussian beam traps," *Phys. Rev. A* **80**, 053808 (2009).
25. S. A. Tatarkova, A. E. Carruthers, and K. Dholakia, "One-Dimensional Optically Bound Arrays of Microscopic Particles," *Phys. Rev. Lett.* **89**, 283901 (2002).
26. E. L. Florin, A. Pralle, E. H. K. Stelzer, and J. K. H. Horber, "Photonic force microscope calibration by thermal noise analysis," *Appl. Phys. A-Materials Sci. & Process.* **66**, S75–S78 (1998).
27. C. D. Mellor and C. D. Bain, "Array formation in evanescent waves," *Chem. Phys. Chem.* **7**, 329–332 (2006).